Small-angle X-ray study of microdomains in rigid PVC

D. J. Blundell
Imperial Chemical Industries Limited, Plastics Division, PO Box 6, Bessemer Road, Welwyn Garden City, Herts, UK
(Received 13 November 1978; revised 15 February 1979)

PVC samples prepared under various conditions have been examined by small-angle X-ray scattering (SAXS) in the region greater than 5 milliradians. The intensity of the scatter is consistent with a two phase structure of crystallites in an amorphous matrix. The scatter profile from the original powder and from mouldings that have not been annealed fits a Debye exponential correlation function. This suggests nodular crystallites of wide size distribution with typical diameters of 3 nm. Mouldings that have been annealed give scattering profiles with a broad peak, whose maximum corresponds to an equivalent Bragg period of about 10 nm. Probably after annealing the nodular crystallites have become more uniform in size and are arranged more regularly.

INTRODUCTION

Morphological structure in PVC has been shown to exist at various levels[1]. Apart from the molecular structure itself, the lowest level consists of microdomains[1] which are typically of the size of 10 nm. In plasticized PVC, there is well-established evidence from electron microscopy that their texture is nodular[2,3]. This evidence is backed by the pronounced small-angle X-ray scattering (SAXS) which shows discrete diffraction maxima that correspond to Bragg spacings of the order of 10 nm[2,3]. It is generally inferred that this periodic spacing is associated with the 'close-packed planes' of a pseudo-hexagonal lattice built up of near-spherical nodules[2]. In rigid PVC, electron microscopical evidence is sparse, although there are clear indications that the nodular structure is still present[3]. SAXS from rigid PVC is weak due to the combination of high absorption and poor electron density contrast. The reason for the stronger SAXS from plasticized PVC is the preferential absorption into the structure by the low electron density plasticizer.

Mos published data on rigid PVC has, in the past, indicated a continuous monotonically-reducing profile with no indication of diffraction maxima that could be associated with structural regularity. Interpretations have differed between those who attribute the scatter to an intrinsic fluctuation in density of the PVC such as a microdomain structure, and those who attribute it to foreign heterogeneities. Neilson and Jabarin[4] associated the scatter with an intrinsic two-phase structure of ordered and disordered regions, without being specific about the nature of the order. Straff and Uhlmann[5] disputed this and assigned the SAXS to surface heterogeneities. Wendorff and Fischer[6] as part of a general investigation of amorphous polymers, suggest heterogeneities in the bulk are the cause. More recently Wenig[7] has reported SAXS profiles with diffraction maxima. It is difficult to explain maxima in terms of a regularity in the structure of a minority heterogeneity; it is much more likely to be due to intrinsic polymer structure. Wenig demonstrated that the profile was consistent with a theoretical model based on small stacks of crystalline lamellae, separated by amorphous regions, where typically there are only two lamellae in each stack. Although this form of structure is common in high crystallinity polymers, it cannot easily be reconciled with the nodular entities seen in electron micrographs.

In the present paper, we report some SAXS studies of rigid PVC that has been subjected to various sample preparation conditions. Both the monotonically reducing profiles and those showing diffraction maxima were observed in this work. In analysing this data, we have deliberately adopted the viewpoint that the scatter is due to an intrinsic two-phase microdomain structure of crystalline and amorphous regions and have set out to find how consistent this model is with the observed profiles.

One problem in dealing with PVC in this way is that although a small proportion (typically 5–10%) of the polymer can be in the crystalline phase, there are indications in the literature that the remaining non-crystalline portions may exist in varous degrees of order with different densities[8]. For simplicity we have ignored this possibility and have assumed a uniform amorphous density.

EXPERIMENTAL

Sample preparation

The following samples were prepared from a PVC suspension polymer powder.

(A) Original powder pressed between glazing plates at about 180°C for 2 min to a thickness of 150–200 μm and then quenched into water.

(B) Powder compounded with stabilizer and granulated into a clear PVC, then pressed as in (A).

(C) Granules of sample B, compression-moulded at 190°C into a sheet 5 mm thick, and then cooled in press to

0032–3861/79/080934–05$02.00

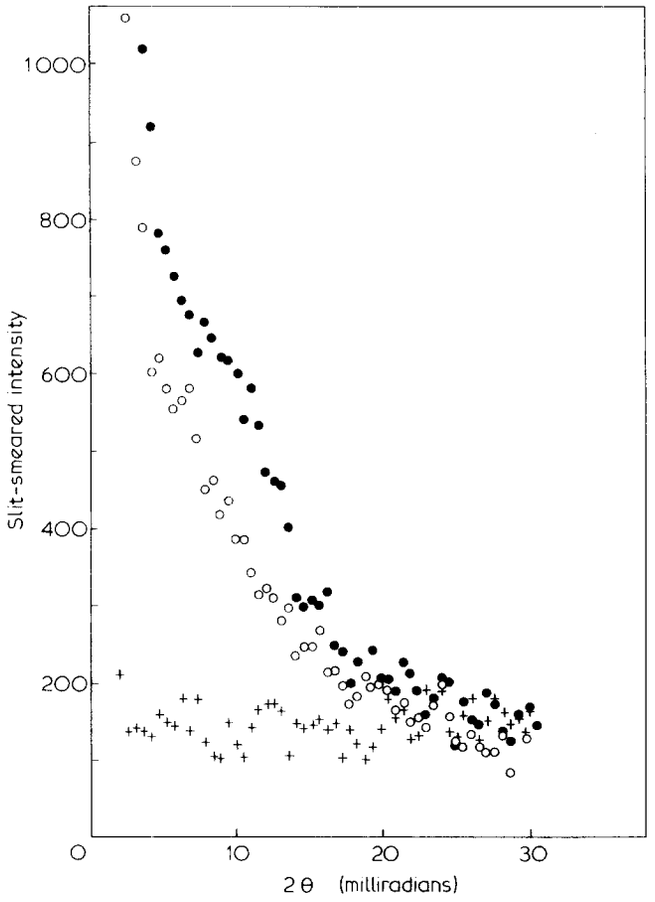

Figure 1 Raw slit-smeared data: ○ = sample B; ● = sample BH; + = amorphous sample

room temperature in 15 min. A 120 μm slice was then cut from the sheet using a 'Microslice' diamond saw.

(D) A thin layer of original powder, wetted by a chlorinated paraffin liquid was smeared on a 12 μm, low crystallinity, polyester support film. This sample was intended for examining powders in their original state without heat treatment. The chlorinated paraffin liquid was chosen to have a close match in electron density and composition to amorphous PVC and should eliminate void scatter. Although at high temperatures this liquid can swell PVC, it is believed that insignificant swelling occurs at room temperature.

(AH) Films of sample A annealed by heating in air at 125°C for 1 h. These conditions are known to enhance crystallinity in PVC[9,10].

(BH) Films of sample (B) annealed in air at 125°C for 1 h.

In addition to these samples, a sample of amorphous PVC supplied by Dr Wenig was also examined. This had been made by 'shock-heating' to 900°C for 15 sec and then quenching[7].

SAXS measurements

The measurements were made on a Kratky low-angle camera (entrance slit 100 μm) using Ni-filtered CuKα radiation. The scatter was detected simultaneously from 2.5 to 90 milliradians using a C. G. R. Linear Position Sensitive Detector and an Elliott Processor Unit which was also equipped with an energy analyser for further monochromatization.

First the transmission factor, T, of each sample was determined. The SAXS was then recorded for 3000 sec. The sample was then removed, and the scatter recorded for (3000 × T) seconds in order to obtain the background radiation, which was then subtracted from the sample profile.

The resulting profile now comprises the 'true' low-angle scatter plus the low-angle tail of the 'fluctuation' scatter. It was assumed that the fluctuation term at low angles was constant with angle and equal to the mean scatter in the region between 60 and 90 milliradians. This constant fluctuation scatter was then subtracted to give the 'true', slit-smeared SAXS profile, $J(s)$.

The intensity was calibrated with a standard 'Lupolen' sample supplied by Professor Kratky's Laboratory. This was used to calculate the Invariant integral

$$\langle \eta^2 \rangle = 2\pi \int_0^\infty J(s) \cdot s \, ds.$$

The data was extrapolated according to the methods of Kortleve and Vonk[11] in order to integrate over the full limits. Invariant integrals for sample type D could not be estimated because of inhomogeneity of the sample.

Estimates of crystallinity index were obtained from wide-angle X-ray diffraction[9,12] using the trace from the amorphous sample as an amorphous template.

RESULTS

Figure 1 shows examples of the raw data after subtraction of the background scatter but before subtraction of the 'constant' fluctuation term. The shock-heated amorphous sample gives level scatter right down to the incident beam stop, indicating the complete absence of any supermolecular structure. The scattering curves from the other samples could be divided into two classes.

Into the first class came samples A, B, C and D which gave monotonically reducing profiles similar to that shown for B in *Figure 1*. There is a slight change of slope at about 5 milliradians suggesting that there are two components of scatter. The scatter above 5 milliradians is due mainly to structure on the scale of 10–20 nm, and can be associated with subprimary particle structure. That seen below 5 milliradians is the tail of the scatter from larger structural units such as primary particles, voids or additives. The presence of two scattering regions agrees with the observations of Neilson and Jabarin[4]. The low-angle camera is not set up to explore the lower angular region.

In the second class were samples AH and BH which gave curves typified by sample BH in *Figure 1*. This curve again shows a change of slope at about 5 milliradians indicating two scattering components. However, unlike the previous curves, the scatter above 5 milliradians now shows a distinct shoulder at about 10 milliradians. This shoulder indicates that there is some degree of order in the structure tending to give a discrete diffraction effect. Different approaches of analysis are needed for these two classes of curves.

The curves with shoulders were analysed to find the Bragg spacing following the general approach used by Geil and coworkers[2,3]. The profile $J(s)$ was first desmeared and then multipled by the Lorentz Factor $4\pi s^2$, where $s = 2 \sin\theta/\lambda$. This results in a profile that is appropriate for the analysis of a one-dimensional periodicity by Bragg's Law. Examples of corrected curves are shown in *Figure 2*, and the Bragg spacings are listed in *Table 1*. It should be noted that profiles that have only been desmeared but have not been

Lorentz corrected also show clear maxima. *Table 1* also lists the estimates of the Invariant $\langle\eta^2\rangle$.

The curves without shoulders were analysed in terms of the 'random two-phase structure' of Debye *et al.*[13,14]. In this approach the structural inhomogeneities in the sample are described by a two point correlation function, $\gamma(r)$.

For a random two-phase structure, Debye *et al.* showed that this function takes the exponential form:

$$\gamma(r) = e^{-r/a}$$

where a is the characteristic length of the structure. The slit-smeared scattered intensity for such a system takes the form[15]:

$$J(s) = \frac{2\pi a^2\langle\eta^2\rangle}{(1+4\pi^2a^2s^2)^{3/2}} \quad (1)$$

According to this relationship, a plot of $J(s)^{-2/3}$ against s^2 should give a straight line, where the ratio of (slope/intercept) can be equated to $4\pi^2a^2$. *Figure 3* shows such a plot for sample B, where it can be seen that the experimental points follow a reasonable linear relationship. The deduced values of a for this class of curve are listed in *Table 1*.

Figure 3 also shows a plot for sample BH, and illustrates that curves with shoulders do not give an acceptable linear Debye relationship and therefore cannot be analysed by this method.

For completeness, the continuous curves were also analysed with the more traditional Guinier plots where it is assumed that the structure consists of particles of one phase dispersed in a matrix of the other phase. In the limit $S \to 0$, Guinier showed that irrespective of particle shape the intensity approaches the asymptotic form[16]:

$$J(s) = J(0)\exp\frac{-4\pi^2S^2R_E^2}{3} \quad (2)$$

where R_E is an average radius of gyration of the particles.

Accordingly $\ln[J(s)]$ was plotted against S^2 and an example for sample B is shown in *Figure 4*.

The data points curve away with increased S^2. This is not unusual for a Guinier plot and is a consequence of the breakdown of the asymptotic form of the Guinier approximation. Attempts were made to estimate R_E in the accepted way by equating the initial slopes for small s (full line in *Figure 4*) to the quantity $-(4\pi^2R_E^{2/3})$. These results are listed in *Table 1*, but because of the curvature their accuracy and significance is open to question.

Trying to reconcile the parameters a and R_E raises a problem in interpretation. In the limit $S \to 0$ the asymptotic form of the Debye equation (1) can itself be approximated to a form which is equivalent to the Guinier equation:

$$J(S) = J(0)\exp -6\pi^2s^2a^2 \quad (3)$$
$$S\to 0$$

Comparing this with equation (2) indicates that the apparent radius of gyration for a system consistent with the Debye form should be $R_E = 2.12a$.

The ratio of R_E/a from the data in *Table 1* is lower than this. The reason is that equation (3) is only a good approxi-

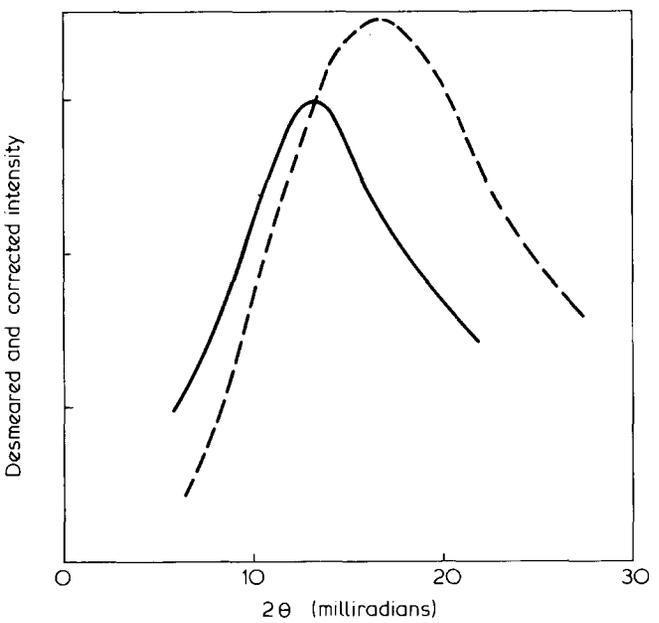

Figure 2 Desmeared and corrected curves of samples annealed at 125°C for 1 h: – – – = sample AH; ——— = sample BH

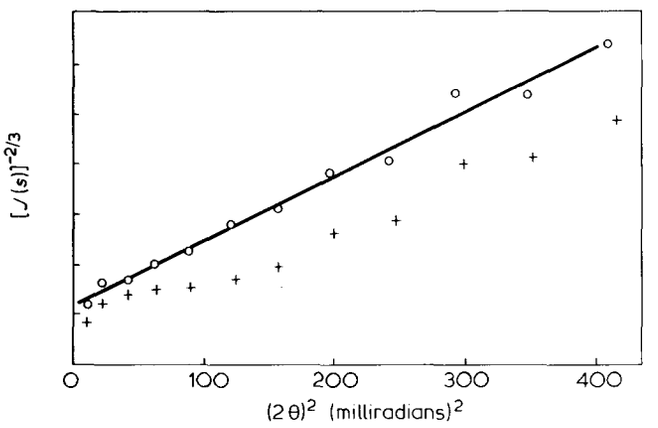

Figure 3 Debye plots of $J^{-2/3}$ *versus* (scattering angle)^2. ○ = sample B; + = sample BH

Table 1

Sample	Correlation length, a (nm)	R_E (nm)	Bragg spacing (nm)	$\langle\eta^2\rangle$ (mole electrons)^2 per cm^3	X-ray crystallinity index, W_c	From equation (1)
A	1.9 ± 0.1	3.3	–	1.9×10^{-4}	≃0.07	0.03
B	2.5 ± 0.1	3.7	–	2.7×10^{-4}	≃0.07	0.04
C	2.1 ± 0.1	3.5	–	5.3×10^{-4}	≃0.10	0.10
D	1.8 ± 0.1	3.2	–	–	–	–
A H	–	–	9.2 ± 0.5	3.0×10^{-4}	≃0.12	0.05
BH	–	–	11.6 ± 0.5	4.4×10^{-4}	≃0.12	0.07

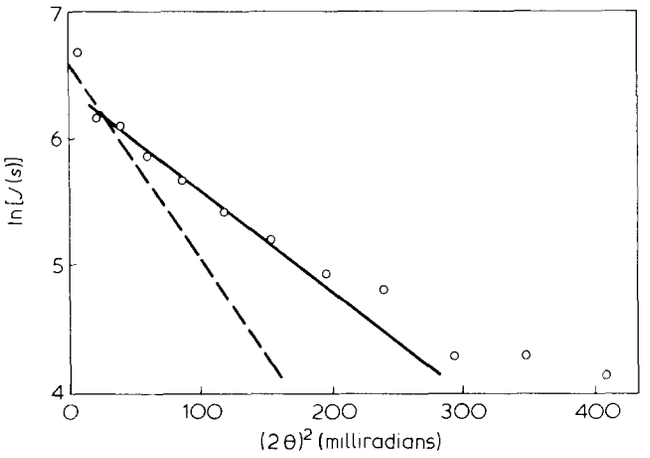

Figure 4 Guinier plot of ln J *versus* (scattering angle)^2 for sample B. Dashed line shows predicted asymptotic behaviour for equation (4) when a = 2.5 nm

mation for equation (1) for a limited range of s below the first significant experimental data points. The broken line in *Figure 4* represents the extrapolation of the asymptotic form (equation 3) using the experimentally deduced value for the Debye parameter a and illustrates the extent of the discrepancy with the full line that was used to deduce the R_E value in *Table 1*. Thus, in choosing between the two methods of analysis, two points of view are possible. Either one assumes that the Debye method is an appropriate description of the structure and that the Guinier plot is misleading because of the poor approximation, or one assumes that the Guinier plot is giving a meaningful value for R_E and that the size and shape of the particulate phase is such as to fortuitously agree with the Debye profile. In the absence of direct microscopical evidence, we favour the Debye approach on the grounds that the formulation is more general and that the data can be fitted over a larger angular range. It should be noted that this approach has worked well on other two phase systems with a nodule-like morphology[18].

DISCUSSION

The most straightforward hypothesis for interpreting the SAXS is that it is due to a two-phase structure consisting of crystalline regions embedded in an amorphous polymer matrix. The magnitude of the Invariant is useful for checking the consistency of this hypothesis. For such a two-phase structure:

$$\langle\eta^2\rangle = \Delta\rho_e^2\phi(1-\phi) \qquad (4)$$

where $\Delta\rho_e$ is the difference in molar electron density between phases and ϕ is the volume fraction of the crystalline phase. If one assumes a crystalline density 1.53 g cm^{-3} [17] and an amorphous density of 1.373 g cm^{-3} [8], then $\Delta\rho_e$ = 0.08 mole electron cm^{-3}. Taking a typical value of 0.1 for ϕ would then give a predicted value of 5.8×10^{-4} for $\langle\eta^2\rangle$. This agrees well with the order of magnitude of the experimental values of $\langle\eta^2\rangle$ and is therefore consistent with the SAXS being due to crystals in an amorphous matrix.

Table 1 lists estimates of ϕ based on equation (4) by assuming $\Delta\rho_e$ = 0.08. These are consistently lower than our estimates of X-ray crystallinity index, W_c. This could either be due to a systematic error in measuring W_c or because the assumed $\Delta\rho_e$ is too high. The value of $\Delta\rho_e$ is based on a crystalline density which was derived from solution grown crystals[17] where the crystal structure could well be more perfect and more dense than those in commercial PVC. Also the amorphous density could be higher than assumed due to molecular ordering[8].

The value for $\langle\eta^2\rangle$ tend to be higher for those samples that have been compounded. This may be due to the additives increasing the effective $\Delta\rho_e$ by reducing the amorphous density. Again, changes in amorphous ordering could also be occurring[8].

The observation of two different classes of diffraction curve indicates that the quality of the morphology of the phase structure depends on the preparation history. The phase arrangement of annealed samples is ordered enough to produce distinct diffraction peaks, which can be analysed in terms of the Bragg spacing.

There are two main ways of interpreting this periodicity. First it can be associated with crystalline lamellar stacks such as those seen in the common crystalline polymers. As such the Bragg spacing should only be taken as a crude estimate of the periodicity and will not correspond to any precise type of average. A more appropriate way of analysing broad peaks in terms of lamellae would be to curve-fit to theoretical models as in the work of Wenig[7]. The alternative approach to interpreting the diffraction peaks is in terms of regularly arranged, near spherical nodules as is suggested by Gezovich and Geil[2], where the Bragg spacing may represent the incipient periodic distance between pseudo-close-packed planes. Present electron microscope evidence[3] would seem to favour this latter interpretation based on a nodular morphology as the most likely.

The interpretation of the continuous scattering curves in terms of the Debye equation does not necessarily imply a picture of extreme randomness. In cases where the properties of phases is imbalanced (as in the crystal/amorphous ratio of PVC) one can normally expect the minor phase to be in the form of particulate inclusions in a matrix of the major phase. This picture would approximate closely to the crystalline nodule structure proposed for the annealed samples. The required randomness would be achieved by a combination of a wide size distribution and an irregular arrangement of nodules.

It follows from the property of the random two-phase model, that the mean chord intercept length L across the nodules is given by:

$$L = \frac{a}{(1-\phi)}$$

If the nodules are spherical then a typical average radius will be

$$r = 3L/4 = \frac{3a}{4(1-\phi)}$$

It is evident therefore from *Table 1*, that the typical nodule size increases from 2.7 nm diameter in virgin powder and powder pressings, to greater than 3 nm diameter in processed PVC. It is interesting to note that this difference in nodule size before and after processing is reflected by the difference in the Bragg spacings in the corresponding annealed samples. This indicates that the memory in the structure due to processing may be carried over into the more ordered structure of the annealed samples.

The equivalent 3 nm spherical diameter is significantly

smaller than the ≃ 10 nm apparent diameter of the nodules seen by electron microscopy on ion-etched surfaces[2]. It should, however, be noted that with crystallinities of 10% and less, the typical distance between the proposed 3 nm crystalline nodules will in fact be nearer 10 nm. Thus it is suspected that the apparent 10 nm diameter is a consequence of the ion-etching defining the locations of the crystallites by preferentially etching the less stable spaces between them.

A related comment can be made concerning the approximate 10 nm Bragg spacing deduced for the annealed samples. If indeed the discrete diffraction is the result of a regularity in packing of crystalline nodules, then for crystallinities of the order of 10%, the nodules must again have a typical diameter of about 3 nm. Thus although the samples have been divided into two classes according to the shape of the diffraction profile, the difference between the morphologies is probably only marginal. Both appear to consist of nodules about 3 nm across, the main difference being mainly in the regularity of their arrangement.

CONCLUSION

The observed SAXS in PVC can be attributed to the two-phase supermolecular structure of crystallites in an amorphous matrix. The arrangement of the crystallites can exhibit various degrees of order. When PVC is annealed under conditions that enhance crystallinity, the order is sufficient to produce a discrete, albeit broad, diffraction peak corresponding to spacings of about 10 nm. It is not possible to tell from SAXS alone whether this peak is the result of a stacked crystalline lamellar morphology or whether it is from semi-ordered arrays of spherical crystalline nodules. *EM* evidence in the literature tends to favour the nodule structure in which case the 10 nm spacing is typical of the internodule distance. Without these annealing conditions, the crystallite arrangement remains disordered and probably consists of irregularly packed nodules with a distribution of sizes. The mean size of the nodules appears to increase with the degree of processing, from typical diameters of 2.7 nm in virgin powder to over 3.0 nm after compounding. The typical distance between nodules remains similar to the 10 nm found in the more regular annealed samples. Thus the microdomain structures of virgin polymer and mouldings, both with and without annealing, all broadly appear to be the same, the main difference being in the higher degree of order in the annealed samples.

ACKNOWLEDGEMENT

We thank Dr W. Wenig for supplying the amorphous 'shock-heated' sample.

REFERENCES

1 Geil, P. H. *J. Macromol. Sci. (B)* 1977, **14**, 171
2 Gezovich, D. M. and Geil, P. H. *Int. J. Polymeric Mater.* 1971, **1**, 3
3 Singleton, C. J., Stephenson, T., Isner, J., Geil, P. H. and Collins, E. A. *J. Macromol. Sci. (B)* 1977, **14**, 29
4 Neilson, G. F. and Jabarin, S. A. *J. Appl. Phys.* 1975, **46**, 1175
5 Straff, R. S. and Uhlmann, D. R. *J. Polymer. Sci. (Polym. Physics Edn)* 1976, **14**, 353
6 Wendorff, J. H. and Fischer, E. W. *Kolloid Z. Z. Polym.* 1973, **251**, 884
7 Wenig, W. *J. Polym. Sci.* to be published
8 Glazkovskii, Yu. V., Zavyalov, A. N., Bakardzhiyer, N. M. and Novak, I. I. *Polym. Sci. USSR* 1971, **12**, 3061
9 Gray, A. and Gilbert, M. *Polymer* 1976, **17**, 44
10 Ohta, S., Kajiyama, T. and Takayanagi, M. *Polym. Eng. Sci.* 1976, **16**, 456
11 Kortleve, G. and Vonk, C. G. *Kolloid Z. Z. Polym.* 1968, **225**, 124
12 Rayner, L. S. and Small, P. A. Br. Pat. 847 676
13 Debye, P. and Bueche, A. M. *J. Appl. Phys.* 1949, **20**, 518
14 Debye, P., Anderson Jr, H. R. and Brumberger, H. *J. Appl. Phys.* 1957, **28**, 679
15 Perret, R. and Ruland, W. *Kolloid Z. Z. Polym.* 1971, **247**, 835
16 Guinier, A. and Fournet, G. 'Small Angle Scattering of X-rays' Wiley, New York, 1955
17 Wilkes, C. E., Folt, V. L. and Krimm, S. *Macromolecules* 1973, **6**, 235
18 Blundell, D. J., Longman, G. W., Wignall, G. D. and Bowden, M. J. *Polymer* 1974, **15**, 33
19 Baur, R. and Gerold, V. *Acta Met.* 1964, **12**, 1448